Stem Cell Reports
Article

OPEN ACCESS

Conditionally Stabilized dCas9 Activator for Controlling Gene Expression in Human Cell Reprogramming and Differentiation

Diego Balboa,[1,4] Jere Weltner,[1,4] Solja Eurola,[1] Ras Trokovic,[1] Kirmo Wartiovaara,[1,3] and Timo Otonkoski[1,2,*]
[1]Research Programs Unit, Molecular Neurology, Biomedicum Stem Cell Center, University of Helsinki, Haartmaninkatu 8, 00290 Helsinki, Finland
[2]Children's Hospital, University of Helsinki and Helsinki University Central Hospital, Stenbäckinkatu 11, 00290 Helsinki, Finland
[3]Clinical Genetics, HUSLAB, Helsinki University Central Hospital, Haartmaninkatu 4, 00290 Helsinki, Finland
[4]Co-first author
*Correspondence: timo.otonkoski@helsinki.fi
http://dx.doi.org/10.1016/j.stemcr.2015.08.001

SUMMARY

CRISPR/Cas9 protein fused to transactivation domains can be used to control gene expression in human cells. In this study, we demonstrate that a dCas9 fusion with repeats of VP16 activator domains can efficiently activate human genes involved in pluripotency in various cell types. This activator in combination with guide RNAs targeted to the *OCT4* promoter can be used to completely replace transgenic OCT4 in human cell reprogramming. Furthermore, we generated a chemically controllable dCas9 activator version by fusion with the dihydrofolate reductase (DHFR) destabilization domain. Finally, we show that the destabilized dCas9 activator can be used to control human pluripotent stem cell differentiation into endodermal lineages.

INTRODUCTION

Clustered regularly interspaced short palindromic repeats (CRISPR)-based systems have recently attracted a lot of attention due to their potential in biotechnological applications. CRISPRs originate from prokaryotic immune response systems and have been engineered to suit genome editing and transcriptional control purposes (Mali et al., 2013a). The most commonly utilized CRISPR system is derived from *Streptococcus pyogenes* and consists of a single CRISPR-associated (Cas) protein, Cas9, and small guide RNAs (gRNAs), either as two separate RNAs or fused into a single chimeric guide RNA. The complex formed by Cas9 and gRNA binds to DNA sequences complementary to the gRNA, upon which the Cas9 protein generates a double-strand break in the DNA. Modified versions of the Cas9 protein have been engineered by mutating important catalytical residues, generating Cas9 proteins that cut only one DNA strand (nickase Cas9) or that are completely inactive (Jinek et al., 2012). Catalytically inactivated Cas9 proteins (dead Cas9, dCas9) can be used to control gene expression, either by physically interfering with the transcription process (Gilbert et al., 2013; Qi et al., 2013) or as fusion proteins with factors that mediate transcriptional repression or activation (Bikard et al., 2013; Cheng et al., 2013; Gilbert et al., 2013; Hu et al., 2014; Maeder et al., 2013a; Mali et al., 2013b; Perez-Pinera et al., 2013). These systems have recently been utilized to mediate target gene activation and repression in mouse and human cells to promote differentiation of human cells (Chavez et al., 2015; Kearns et al., 2014) and transdifferentiation and reprogramming of mouse cells (Chakraborty et al., 2014; Gao et al., 2014). Moreover, various externally controllable Cas9 proteins have recently been described for gene editing using split Cas9 architecture with either rapamycin-inducible dimerization domains (Zetsche et al., 2015) or tamoxifen-dependent intein splicing (Davis et al., 2015).

In this study, we describe an efficient dCas9 activator with multimeric VP16 activation domain and a simplified method for guide RNA assembly and cloning. We demonstrate that the dCas9 activator can be fused to a dihydrofolate reductase (DHFR)-derived destabilization domain (DD) (Iwamoto et al., 2010) and used to control gene expression with addition of Trimethoprim (TMP) in multiple human cell types. Furthermore, we demonstrate that the dCas9 activator can be used to replace transgenic OCT4 in human cell reprogramming and that human pluripotent cell differentiation can be induced by the activator in a TMP-dependent manner.

RESULTS

dCas9-Transactivator Optimization for Induction of *OCT4* Expression

We introduced a second mutation to the previously published nicking version of humanized *Streptococcus pyogenes* Cas9 (Cong et al., 2013) to incorporate both D10A and H840A mutations that render it catalytically inactive (dCas9). This protein was then C-terminally fused with three repeats of the PADALDDFDLDML sequence of the Herpes simplex virus protein 16 (VP16) transactivation domain (Baron et al., 1997), generating the dCas9VP48 activator version. The function of the construct was validated in reporter HEK293 cells, where GFP expression is

under the control of TetON promoter. After targeting dCas9VP48 to the TetON promoter with different gRNAs, we observed increased number of GFP-positive cells in the condition with TetOp2 gRNA, which binds four times to the TetON promoter sequence (Figure S1). Thus, dCas9VP48 showed transcriptional activation activity when targeted multiple times to a promoter sequence.

Most studies so far have used dCas9 activators with VP16 transactivation sequences repeated between three and ten times (Cheng et al., 2013; Maeder et al., 2013a; Mali et al., 2013b; Perez-Pinera et al., 2013). To test the effect of increasing the number of VP16 repeat domains, we cloned additional constructs with 6 and 12 repeats of the VP16 sequence (hereafter referred to as dCas9VP96 and dCas9VP192 accordingly) (Figure 1A) and targeted the endogenous *OCT4* (*POU5F1*) promoter proximal area in HEK293 cells using five gRNAs. Efficient *OCT4* upregulation was detected both at mRNA and protein level (Figures 1B and 1C). As dCas9VP192 caused the highest increase in *OCT4* expression levels, up to 70-fold, it was used for further experiments.

dCas9VP192-Assisted Transcriptional Activation of Pluripotency Genes

We next tested the upregulation of additional endogenous pluripotency genes *SOX2*, *NANOG*, *LIN28*, *KLF4*, and *CDH1* (E-Cadherin) in HEK293 cells by targeting dCas9VP192 to their promoters with five different gRNAs. Single gRNA transcriptional units were assembled by PCR and pooled and transfected together with dCas9VP192 encoding plasmid (Figure 1D). Expression of targeted endogenous factors could be detected by immunocytochemistry 72 hr after transfection (Figure 1E). PCR-gRNA fragments were then concatenated and cloned into plasmids using Golden Gate assembly (Figure 1D) and tested by transfection into HEK293 cells. Immunocytochemistry and qRT-PCR analysis showed activation of the endogenous-targeted genes (Figures 1F and 1G). *OCT4*, *SOX2*, *NANOG*, and *CDH1* transcription was upregulated more than 20-fold over basal levels. *LIN28* and *KLF4* activation was more modest, possibly indicating either a less permissive chromatin state in the promoter of these genes or a high basal expression in HEK293 cells. These results showed that our method enables rapid testing of many gRNA candidates, which are easily generated with a single PCR. The subsequent concatenation of the successful ones in a single-step reaction allows for easy cloning of the guides into varying vectors.

To study the ability of the gRNA-encoding plasmids and the dCas9VP192 to activate gene expression in human skin fibroblasts, we cloned the dCas9VP192 activator and the concatenated guides into transiently replicating OriP-EBNA1-containing plasmids (Okita et al., 2011). Human skin fibroblasts were electroporated with dCas9VP192-EBNA and gRNA-encoding-EBNA plasmids. Activation of endogenous *OCT4*, *SOX2*, and *LIN28A* but not *NANOG* could be detected in cells 6 days after electroporation by immunocytochemistry and *OCT4* and *SOX2* activation by qRT-PCR (Figures 2A–2C).

Reprogramming Factor OCT4 Replaced by dCas9VP192-Mediated Gene Activation

It has been previously demonstrated that dCas9 activators containing between four and ten VP16 repeats can be used to replace transgenic Oct4 in mouse fibroblast reprogramming by targeting the *Oct4* distal enhancer (Gao et al., 2014). To determine whether dCas9VP192-mediated *OCT4* activation would work in human cell reprogramming, we substituted the transgenic OCT4 plasmid in the episomal reprogramming protocol by dCas9VP192 and *OCT4* promoter targeting guides (Okita et al., 2011; Yu et al., 2009) (Figure 2D). Activation of endogenous *OCT4* could be detected in electroporated human skin fibroblasts expressing the dominant-negative form of p53 by day 6 of reprogramming (Figure 2E). Early colonies formed by day 9 of reprogramming and classical alkaline phosphatase positive (AP+) iPSC colonies were detected by day 18 (Figure 2F). Control conditions, where OCT4 guide plasmid had been replaced with GFP encoding plasmid, did not result in AP+ colony formation or endogenous *OCT4* activation (Figure 2E).

We cloned short hairpin RNA for p53 into the dCas9VP192 plasmid to enable transient p53 inhibition in healthy fibroblasts during reprogramming. To compare the reprogramming efficiency of dCas9VP192-mediated endogenous *OCT4* activation to transgenic OCT4 expression, we electroporated adult human skin fibroblasts with the reprogramming constructs and assessed the reprogramming efficiency by colony morphology and AP positivity. The colony formation efficiency was not found to differ significantly between the methods (0.0054% of plated cells for *OCT4* activation versus 0.0021% for transgenic OCT4) (Figure 2G). Using sh-p53-dCas9VP192 construct and *OCT4* targeting guides instead of exogenous OCT4 plasmid, we successfully derived iPSC from skin fibroblasts obtained from a 14-year-old donor with permanent neonatal diabetes mellitus (PNDM) and from a healthy 72-year-old donor (F72) (Figures S2A and S2B). The derived iPSC colonies were propagated for at least ten passages. All iPSC colonies expressed OCT4, NANOG, TRA-1-60, and TRA-1-81 (Figure 2H), and qRT-PCR analysis verified the expression of additional pluripotency markers (Figure S2A). iPSC lines were able to differentiate into the three germline derivatives positive for FOXA2 (endoderm), VIMENTIN (mesoderm), and βIII-TUBULIN (ectoderm) in embryoid bodies (Figure 2I). Clearance of the episomal reprogramming plasmids was confirmed in 12 of 17 iPSC clones in

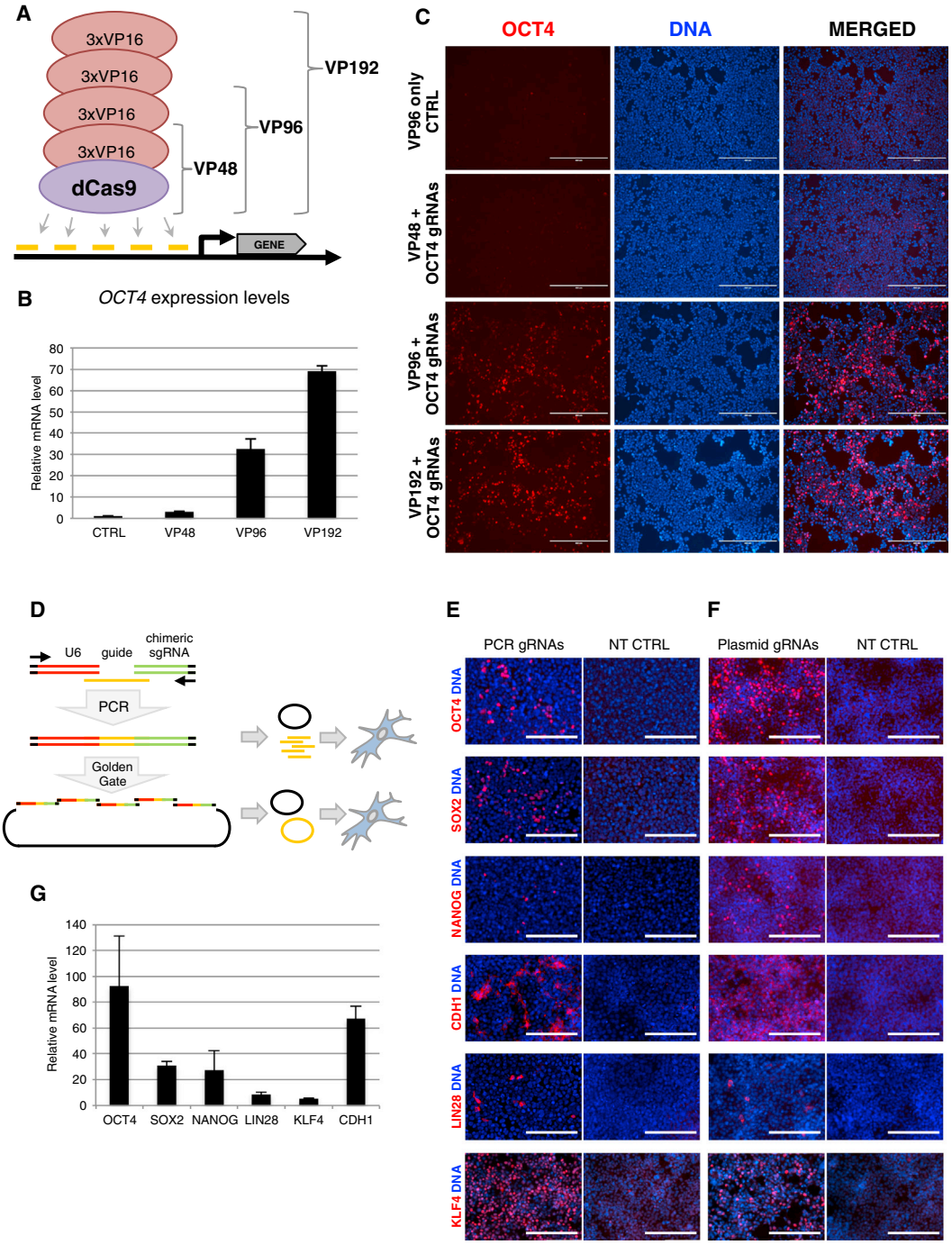

Figure 1. Strategy for dCas9-Mediated Activation of Pluripotency Genes

(A) Schematic representation of dCas9 activator versions tested.

(B) Upregulation of *OCT4* in HEK293 cells by different dCas9 activator versions. Relative mRNA expression levels were measured by qRT-PCR 72 hr after transfection. VP96-only transfection was used as control. Data represent mean ± SEM, n = 5 independent transfections.

(C) Immunocytochemical analysis of OCT4 in HEK293 cells 72 hr after transfection with dCas9 activator versions and *OCT4* targeting gRNAs. Scale bars represent 400 μm.

(D) Schematic representation of the gRNA cloning and testing strategy. gRNAs were first validated with PCR-amplified fragments before concatenating them into plasmids by Golden Gate assembly.

(legend continued on next page)

passage 2 (Figure S2B). Thus, human skin fibroblasts can be reprogrammed into iPSC by replacing OCT4 overexpression with dCas9 activator-mediated activation of endogenous *OCT4*.

Conditionally Stabilized dCas9 Activator

In order to control temporally the activity of the dCas9 activator, we fused the protein N-terminally to the *E. coli*-derived DHFR DD. This allowed us to control the stability of the activator in a TMP-dependent manner (Figure 3A). To test the construct in gene activation, we initially created a destabilized version of the dCas9VP48 activator (DDdCas9VP48) and generated HEK293 cells constitutively expressing DDdCas9VP48 with and without *OCT4* targeting guides. In the absence of guides, OCT4 expression was not detected in the cells (Figure S3A). In the presence of guides, only some leaky OCT4 expression could be detected in a minor population of cells, which was drastically increased upon addition of TMP (Figure S3A).

To compare the TMP-inducible dCas9 system with the more commonly used doxycycline inducible TetON system, we generated stable HEK293 cell lines with TetON-dCas9VP192, constitutive DDdCas9VP192, or TetON-DDdCas9VP192 and guides targeting the *OCT4* promoter. Both TetON-dCas9VP192 and DDdCas9VP192 performed comparably (Figures 3B and 3C), presenting leaky expression at non-induced d0 samples, and upregulation of *OCT4* after addition of doxycycline or TMP, to up to 5.2 and 6.6 times the expression levels of human embryonic stem cells (hESCs) accordingly. The combination of both TetON promoter and DHFR DD with the dCas9VP192 eliminated the nonspecific activation of *OCT4* in the absence of doxycycline or TMP (Figures 3B and 3C).

We then generated HEK293 cells constitutively expressing the DDdCas9VP192 activator and guides targeting *OCT4*, *SOX2*, *NANOG*, and *LIN28A* promoters simultaneously. Some leaky activation of *OCT4* and *SOX2* but not *NANOG* or *LIN28A* could be detected in cells not treated with TMP (Figure 3D). After addition of TMP, the expression of *OCT4*, *SOX2*, and *NANOG* increased already by day 1, reaching 24%, 187%, and 41% of the expression levels measured in hESC (H9), respectively (Figure 3D). In contrast to the other factors, *LIN28A* upregulation was not detected by qRT-PCR (Figure 3D). Unlike the strongly activated OCT4, LIN28A expression could be detected in only a few cells by immunocytochemistry (Figure 3E).

To test the activator in primary human cells, we generated F72 human skin fibroblasts constitutively expressing the DDdCas9VP192 and *OCT4*, *SOX2*, *NANOG*, and *LIN28A* promoter targeting guides. Leaky activation was not detected in the fibroblasts in the absence of TMP (d0, Figures 3F and 3G). In the presence of TMP, *OCT4*, *SOX2*, and *NANOG* expression rose gradually reaching highest expression of 46%, 63%, and 7% of hESC levels, respectively, by the end of the 9-day period (Figure 3F). *LIN28A* upregulation was not robustly detected by qRT-PCR in fibroblasts (Figure 3F), but rare positive cells could be detected by immunocytochemistry (Figure 3G).

In an attempt to improve the activation efficiency of the target genes in the fibroblasts, we tested a set of inhibitors commonly used for iPSC induction to explore whether chemical compounds could improve dCas9VP192-mediated gene activation. However, treatment with these inhibitors did not significantly increase target gene activation efficiency (Figures S3B–S3D).

Activation of Endodermal and Pancreatic Transcription Factors by dCas9VP192

In order to examine the versatility of our method in activating different genes, we targeted a set of endodermal and pancreatic master transcription factors with dCas9VP192. We designed gRNAs targeting the proximal promoters of *FOXA2*, *SOX17*, *GATA4*, *PDX1*, and *NKX6.1*, PCR-amplified and tested them as described above. After preliminary confirmation of gene activation by immunocytochemistry, gRNAs were concatenated and validated in HEK293 cells. Analysis at 72 hr after transfection showed clear activation of the tested genes at the protein and mRNA level (Figure S4A).

Activation of endodermal transcription factor SOX17 using a dCas9 activator has been reported to work efficiently in hESCs (Kearns et al., 2014). To address whether our set of genes could be upregulated by dCas9VP192 in pluripotent stem cells, we transfected dCas9VP192 plus gRNA-encoding plasmids to human iPSCs. After 72 hr, activation of all the five tested genes was detected by immunocytochemistry and confirmed by qRT-PCR (Figures 4A, 4B, and S4C), demonstrating that dCas9VP192 can drive the expression of differentiation-relevant transcription factors also in pluripotent cells.

Next we generated a hESC line (H9) constitutively expressing DDdCas9VP192 activator and gRNAs targeting

(E) Immunocytochemical detection of the products of the targeted genes in HEK293 cells 72 hr after transfection with PCR gRNA fragments and dCas9VP192 plasmid. Non-treated (NT) HEK293 cells were used as staining control. Scale bars represent 200 μm.

(F) Activation of targeted genes in HEK293 cells transfected with gRNA-concatenated plasmids and dCas9VP192 plasmid. Scale bars represent 200 μm.

(G) Upregulation of mRNA levels of targeted genes measured by qRT-PCR in HEK293 cells 72 hr after transfection with gRNA-concatenated plasmids and dCas9VP192 plasmid. Data represent mean ± SEM, n = 2–4 independent transfections.

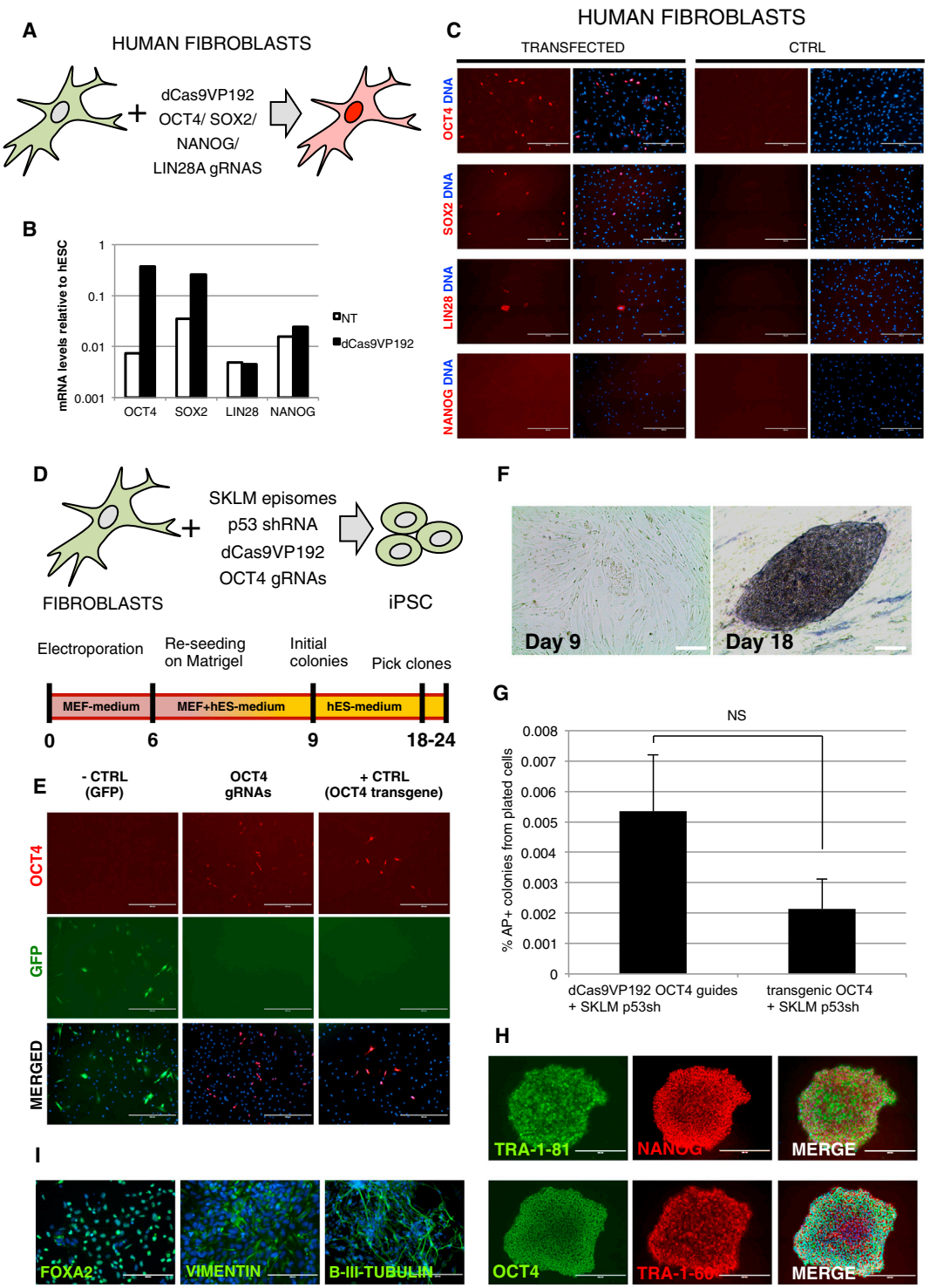

Figure 2. Functional Validation of dCas9 Activator in Reprogramming to Pluripotency

(A) Schematic representation of factors targeted in human skin fibroblasts with the dCasVP192 in transient electroporation.

(B and C) qRT-PCR and immunocytochemical detection of the targeted pluripotency factors 6 days after electroporation of human skin fibroblasts with dCas9VP192-EBNA and gRNA-encoding-EBNA. Scale bars represent 400 μm.

(D) Schematic representation of factors used in OCT4 replacement reprogramming protocol.

(legend continued on next page)

the endodermal transcription factors *FOXA2* and *SOX17* and the pancreatic factors *PDX1* and *NKX6.1* to test the applicability of this system in directed differentiation. The H9-DDdCas9VP192 cells were treated for 3 days following an endodermal differentiation protocol (Rezania et al., 2014) (Supplemental Experimental Procedures) either in the complete medium including Activin A (AA) (−TMP +AA condition), without Activin A as a control (−TMP −AA), or with 1 μM TMP and no Activin A (+TMP −AA) (Figure 4C). As expected, the cells treated for 3 days with AA differentiated into FOXA2$^+$/SOX17$^+$ definitive endoderm but did not express pancreatic progenitor marker genes (Figures 4D and S4D). In contrast, the simultaneous activation of endodermal and pancreatic transcription factors upon the addition of TMP upregulated pancreatic progenitor markers in the same time period. These cells expressed FOXA2, SOX17, PDX1, and NKX6.1 directly activated by DDdCas9VP192 (Figures 4D, 4E, and S4D). Importantly, also their downstream target transcription factors SOX9 and NKX2.2 were induced at both the mRNA and protein levels (Figures 4D and 4E).

To demonstrate the feasibility of using DDdCas9VP192 target gene activation in combination with other inducible expression systems, we generated a transgenic hESC line expressing DDdCas9VP192 activator, gRNAs targeting the pancreatic transcription factors *PDX1* and *NKX6.1*, and a doxycycline-inducible overexpression cassette for mature beta cell transcription factor MAFA (TetON-MAFA-ires-GFP). The cells were treated with a pancreatic differentiation protocol for 9 days (Rezania et al., 2014). The experimental protocol is presented in Figure 4F. From days 3 to 9, the cells were treated with 1 μM TMP to induce *PDX1* and *NKX6.1* expression and from day 7 to 9 with 1 μg/ml doxycycline to induce MAFA (Figure 4F). At both days 7 and 9 of differentiation, *PDX1* and *NKX6.1* expression levels were increased in the +TMP condition, as shown by qRT-PCR and immunocytochemistry (Figures 4G and 4H). MAFA overexpression was robustly detected in the doxycycline-treated conditions at day 9, together with the upregulation of MAFA downstream target glucokinase (GCK) (Figures 4G and 4H) (Wang et al., 2007). These results demonstrate that the two inducible systems can be combined to control the expression of specific genes at distinct time points of the differentiation process.

Finally, we also tested these constructs in primary human foreskin fibroblasts. Endogenous gene activation was detected at protein and mRNA level (Figure S4B), albeit at low efficiency, indicating that dCas9VP192 can activate endodermal gene transcription even in somatic cells with a more restrictive epigenetic landscape.

DISCUSSION

We report on the ability of dCas9 activators to upregulate the expression of endogenous human genes associated with reprogramming and maintenance of pluripotency as well as differentiation. We optimized the dCas9 activator efficiency and described a simplified workflow for testing and cloning the guide RNAs. The potent functional effect of the dCas9VP192 was demonstrated by replacing transgenic OCT4 with the activator in the reprogramming of primary human fibroblasts into iPSCs. Furthermore, we converted the activator into a conditionally stabilized version, which can be controlled by a small molecular compound, and demonstrated its function in controlling cell differentiation.

Our results show that increasing the number of VP16 transactivator repeats fused to dCas9 leads to improved activation of the endogenous *OCT4*. Using dCas9VP192 and five gRNAs, we obtained up to 70-fold *OCT4* upregulation in HEK293 cells, in similar range of efficiency with previous studies (Cheng et al., 2013; Hu et al., 2014; Mali et al., 2013b). The fact that dCas9 activators can replace transgenic OCT4 as a reprogramming factor in human iPSC derivation speaks for the functional relevance of the gene activation and the potential for utilizing this approach for human cell type conversions. A similar approach has

(E) Immunocytochemical detection of activation of endogenous *OCT4* in human skin fibroblasts on day 6 of reprogramming. Cells were electroporated with pCXLE-GFP (-CTRL), episomal SOX2, KLF4, LIN28, and L-MYC plus dCas9VP192 and either OCT4 gRNAs plasmid or pCXLE-OCT4 (+CTRL). Scale bars represent 400 μm.

(F) Formation of AP+ colonies with dCas9VP192 replacing transgenic OCT4. Scale bars represent 200 μm.

(G) Comparison of episomal reprogramming efficiencies of adult human skin fibroblasts using either dCas9VP192 and *OCT4* targeting guides or transgenic OCT4 together with transgenic SOX2, KLF4, LIN28, L-MYC, and p53 shRNA. Data represent mean ± SEM, n = 4 independent experiments, p = 0.177 using Student's t test.

(H) Immunocytochemical detection of pluripotency markers TRA-1-81, NANOG, OCT4, and TRA-1-60 in passage 2 iPSCs derived from normal human fibroblasts with transgenic OCT4 replacement by dCas9VP192 and SKLM transgenes. Scale bars represent 400 μm.

(I) Immunocytochemical detection of markers of different germ layers in plated embryoid bodies of iPSCs derived from PNDM human fibroblasts by transgenic OCT4 replacement using dCas9VP192.FOXA2 (endoderm), VIMENTIN (mesoderm), and βIII-TUBULIN (ectoderm). Scale bars represent 200 μm for VIMENTIN.

See also Figure S2.

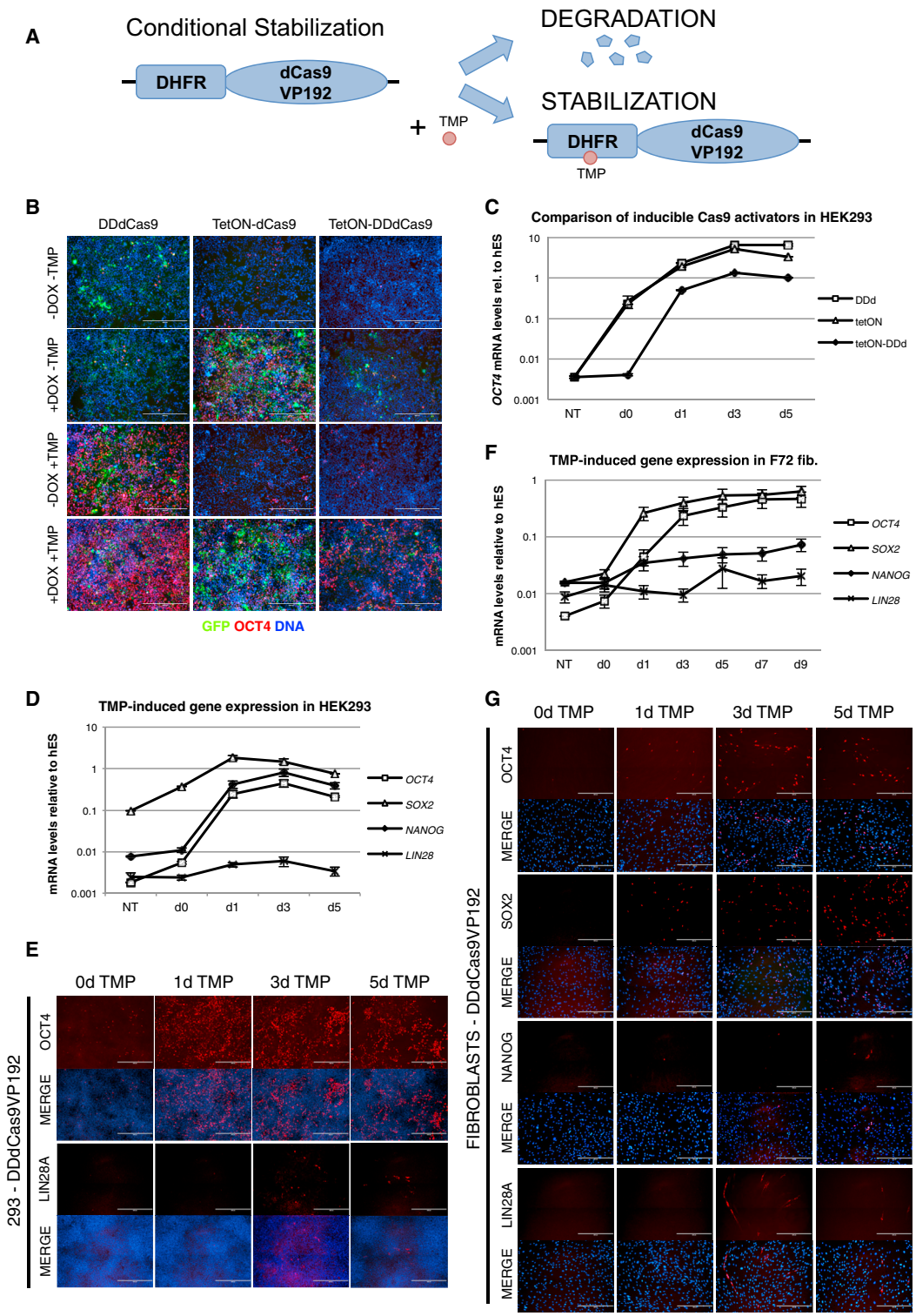

Figure 3. Gene Activation by Conditionally Stabilized dCas9VP192

(A) Schematic representation of DDdCas9VP192 stabilization. TMP, Trimethoprim.

(B) Immunocytochemical staining for OCT4 activation in selected HEK293 cells expressing DDdCas9VP192-T2A-GFP, TetON-dCas9VP192-T2A-GFP, or TetON-DDdCas9VP192-T2A-GFP activators and *OCT4* targeting guides in the presence or absence of TMP and doxycycline. Scale bars represent 400 μm.

(legend continued on next page)

been previously demonstrated to work for mouse cell reprogramming (Chakraborty et al., 2014; Gao et al., 2014).

The potency of dCas9 activators varies between genes. We were not able to efficiently replace additional reprogramming factors, although their activation could be detected in fibroblasts. As NANOG and LIN28A activation was detected only in a minor population of cells, it is likely that the activation of these genes is stochastic by nature and limited by epigenetic barriers. Therefore, alternative approaches, for example, improved transactivation domains or catalytically active domains affecting the epigenetic state of the gene regions may be needed (Chavez et al., 2015; Hilton et al., 2015; Konermann et al., 2015; Maeder et al., 2013b). Additionally, the size of the construct could be reduced by incorporating multimerization sites for the activator domains, such as the recently reported SunTag peptide tail, which would implement an amplification step in the recruitment of transactivators to the proximal promoter that results in greatly enhanced gene activation (Tanenbaum et al., 2014). Targeting noncoding RNAs as well as genomic enhancer elements in addition to promoter proximal areas might also help in replacing transgenic factors with only dCas9 activators and gRNAs (Gao et al., 2014; Hilton et al., 2015).

The power of the dCas9 system for affecting gene expression lies in the multiplexing potential of the short gRNA sequences. Concatenation of gRNA expression cassettes using Golden Gate cloning has recently been described for multiplex genome editing (Sakuma et al., 2014) and gene activation (Kabadi et al., 2014). In contrast, our method avoids time-consuming traditional cloning for the initial gRNA-assembly step, being substituted by a simple PCR reaction. After gRNA efficiency validation, the gRNA-PCR fragments are concatenated with a single Golden Gate reaction, streamlining the generation of gRNA-encoding plasmids for different target genes. The small size of the gRNA construct compared with transgenic expression methods allows for efficient simultaneous targeting of multiple genomic loci and potentially full gene regulatory networks (GRNs). As dCas9 activators are targeting the endogenous genes for activation, activation of the proximal regulatory regions might benefit the establishment of proper transcriptional programs by affecting epigenetic barriers to the reprogramming process.

N-terminal fusion of the dCas9 activator with the DHFR DD leads to a functional TMP-dependent dCas9 activation. In terms of inducible gene transcription, DDdCas9 activator performs as efficiently as the TetON dCas9, with the advantage of not requiring an additional rtTA transactivator element. The DDdCas9 activator did, however, show a certain level of leakiness possibly due to incomplete protein degradation. This nonspecific activation can be controlled by combining the DDdCas9 activator with additional inducible systems like TetON, as shown in Figure 3B, or by controlling the expression level of the activator. Moreover, combining the *S. pyogenes* DDdCas9 activator with other orthogonal Cas9-derived conditional transcriptional modulators should allow for simultaneous temporal control over multiple gene expression programs (Davis et al., 2015; Esvelt et al., 2013; Ran et al., 2015; Zetsche et al., 2015).

Kearns et al. (2014) demonstrated that dCas9 transcriptional activators and repressors can be used to control human pluripotent stem cell differentiation by targeting endogenous *SOX17* and *OCT4*. We have expanded the target gene list to additional key factors in the endodermal and pancreatic differentiation pathways. The induction of these genes may accelerate the differentiation of pluripotent stem cells to pancreatic progenitor-like cells to only 3 days, as compared with 10 or more days needed with current differentiation protocols (Rezania et al., 2014). The expression in these cells of genes downstream of FOXA2, SOX17, PDX1, and NKX6.1 indicates that simultaneous activation of a key gene set by DDdCas9 activator could help in establishing cell-type-specific GRNs (Arda et al., 2013). This constitutes a method to study and improve the differentiation of pluripotent stem cells to a particular lineage, for example, by activation of key regulators of lineage bifurcations or terminal differentiation. Moreover, DDdCas9-mediated transcriptional activation of genes can be utilized in combination with well-established overexpression methods, as we show here for doxycycline-inducible systems, adding an extra layer of tunable and temporally controlled gene expression.

(C) Comparison of inducible DDdCas9, TetON-dCas9, and TetON-DDdCas9 activators in the upregulation of *OCT4* levels in HEK293 cells. Cells were treated for up to 5 days with 1 μM TMP (for DDdCas9), 1 μg/ml of doxycycline (for TetON-dCas9), or both (for TetON-DDdCas9). Expression levels relative to H9 hESC are represented as mean ± SEM, n = 3 independently treated samples.

(D and E) Temporal activation of *OCT4*, *SOX2 NANOG*, and *LIN28A* induced with 1 μM TMP analyzed by qRT-PCR and OCT4 and LIN28A by immunocytochemistry in HEK293 cells expressing DDdCas9VP192 and gRNAs targeting these genes. Expression levels relative to H9 hESC are represented as mean ± SEM, n = 4 independently treated samples. Scale bars represent 400 μm.

(F and G) Temporal activation of *OCT4*, *SOX2 NANOG*, and *LIN28A* induced with 1 μM TMP analyzed by qRT-PCR and immunocytochemistry in primary human skin fibroblasts (F72) expressing DDdCas9VP192 and gRNAs targeting these genes. Expression levels relative to H9 hESC represented as mean ± SEM, n = 4 independently treated samples. Scale bars represent 400 μm.

See also Figure S3.

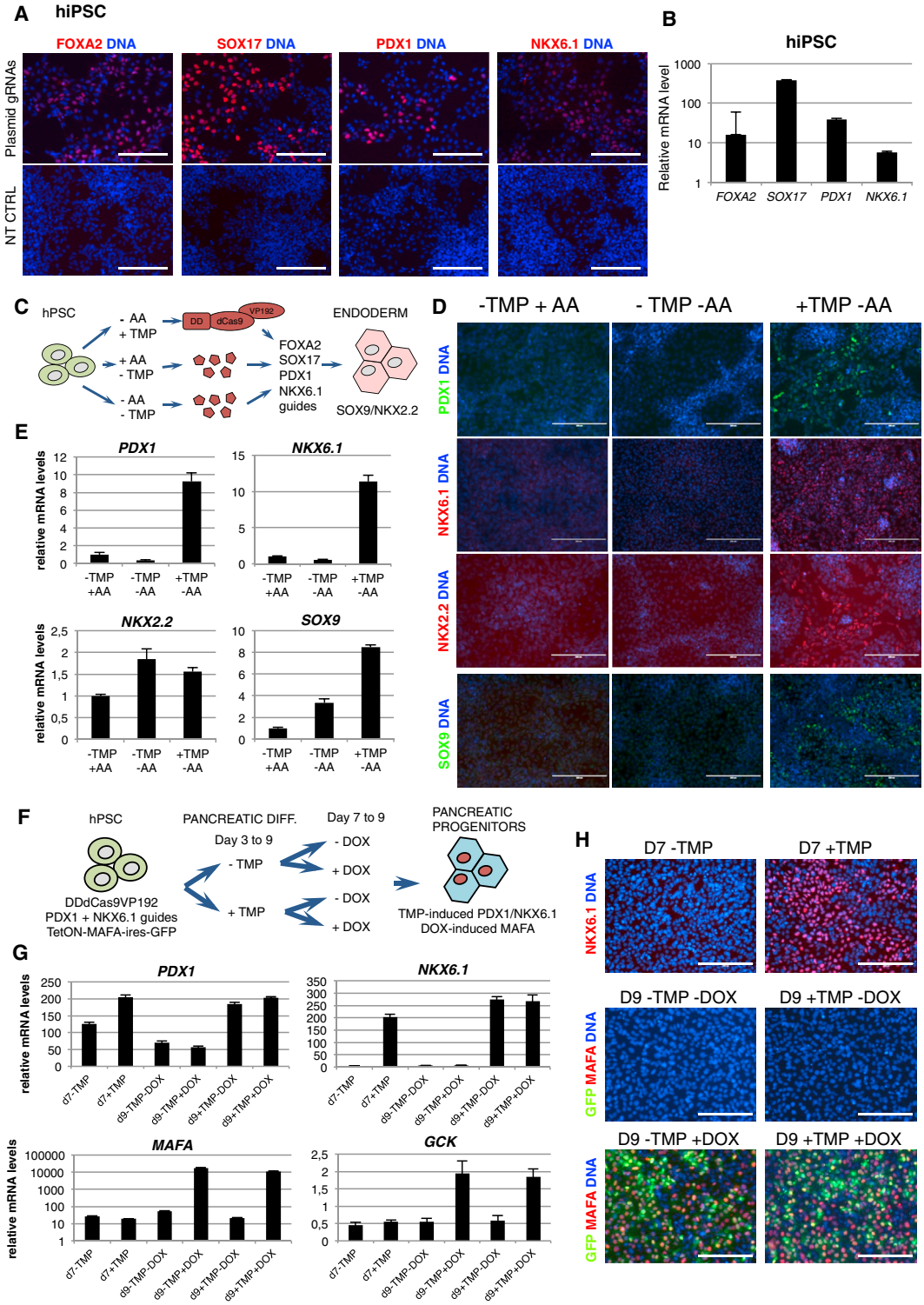

Figure 4. Activation of Lineage-Specific Transcription Factors by dCas9VP192

(A) Immunocytochemical detection of dCas9VP192 targeted endodermal and pancreatic genes in hiPSC line HEL72.1. Scale bars represent 200 μm.

(B) qRT-PCR analysis of indicated targeted genes in hiPSC. Data represent mean ± SEM relative to non-transfected cells, n = 2 independent transfections. Analyses in (A) and (B) were performed 72 hr after delivery of gRNA-concatenated plasmids and dCas9VP192.

(legend continued on next page)

In the future, combining the dCas9 activators with large-scale nucleic acid synthesis and high-throughput screening may enable the generation of gRNA arrays to activate simultaneously a determined set of genes (e.g., all the key components in a GRN), providing an unprecedented level of precision for controlling cellular reprogramming and differentiation (Gilbert et al., 2014; Shalem et al., 2014; Wang et al., 2014).

EXPERIMENTAL PROCEDURES

Ethical Consent

The generation of the human induced pluripotent stem cell (hiPSC) lines used in this study was approved by the Coordinating Ethics Committee of the Helsinki and Uusimaa Hospital District (Nro 423/13/03/00/08).

Cell Culture

HEK293 cells, skin fibroblasts derived from a 14-year-old donor with PNDM, healthy 72-year-old skin fibroblast (F72), and human foreskin fibroblasts (HFFs, ATCC line CRL-2429) were cultured in fibroblast medium (DMEM; Life Technologies) containing 10% fetal bovine serum (FBS; Life Technologies), 2 mM GlutaMAX (Life Technologies), and 100 g/ml penicillin-streptomycin (Sigma). hESC and hiPSCs were cultured on Matrigel-coated dishes in E8 medium (Life Technologies, A1517001) in an incubator at 37°C and 5% CO_2. The HEL72.1 hiPSC cell line was retrovirally derived from PNDM-patient fibroblasts, and in vitro differentiation through embryoid bodies was performed as described elsewhere (Vuoristo et al., 2013).

Guide RNA Design and Production

Guide RNA sequences were designed using the http://crispr.mit.edu web-based tool, targeting them to the proximal promoters (−400 to −50 base pairs from transcription start site) of the gene of interest. Possible guides were selected according to their off-target score and position. Guide RNA transcriptional units (gRNA-PCR) were prepared by PCR amplification and further concatenated using Golden Gate assembly. See Supplemental Experimental Procedures for further details.

Pluripotent Reprogramming

For human skin fibroblast reprogramming, 1 million cells were electroporated with Neon electroporator (Life Technologies), as described in Supplemental Experimental Procedures. A total of 6 μg of DNA was used per electroporation, containing 2 μg of pCXLE-dCas9VP192-GFP-shp53 and 1 μg of each other plasmids (guide encoding EBNA plasmids and reprogramming plasmids pCXLE-OCT4, pCXLE-hSK, and pCXLE-hUL). Afterward, electroporated cells were plated on gelatin-coated tissue culture dishes in fibroblast medium. On day 6, electroporated cells were split onto Matrigel-coated plates and cell culture medium was changed to a 3:1 mixture of hES and fibroblast-medium. After initial colony formation, the medium was changed to hES-medium (KnockOut DMEM; Life Technologies) supplemented with 20% knockout (KO) serum replacement (Life Technologies), 1% GlutaMAX, 0.1 mM beta-mercaptoethanol, 1% nonessential amino acids (Life Technologies), and 6 ng/ml basic fibroblast growth factor (bFGF, Life Technologies) supplemented with 0.25 mM sodium butyrate (NaB; Sigma). Medium was changed every other day. Emerging iPSC colonies were picked on Matrigel-coated dishes in E8 medium. P53 defective HFFs used in guide testing were infected with dominant-negative p53DD-encoding retrovirus (Addgene plasmid: 22729) and passaged twice before reprogramming. Clearance of episomal plasmids was demonstrated by PCR (Okita et al., 2011).

SUPPLEMENTAL INFORMATION

Supplemental Information includes Supplemental Experimental Procedures and four figures and can be found with this article online at http://dx.doi.org/10.1016/j.stemcr.2015.08.001.

AUTHOR CONTRIBUTIONS

D.B. and J.W. conceived the study and designed the experiments. D.B., J.W., and S.E. performed the experiments and analyzed the data. D.B., J.W., and T.O. wrote the manuscript with input from R.T. and K.W. T.O. provided funding for the work.

ACKNOWLEDGMENTS

We thank Eila Korhonen and Heli Mononen for technical assistance. We are grateful to Alejandro Sarrión-Perdigones (Baylor

(C) Schematic representation of DDdCas9VP192-mediated activation of endodermal and pancreatic genes for differentiation of hiPSC.
(D) Immunocytochemistry of hESC H9 expressing DDdCas9VP192 and gRNAs for *FOXA2*, *SOX17*, *PDX1*, and *NKX6.1* differentiated to definitive endoderm at day 3. hESC treated with 100 ng/ml Activin A (−TMP +AA), basal medium control (−TMP −AA) and basal medium with 1 μM TMP (+TMP −AA) stained for pancreatic progenitor markers PDX1, NKX6.1 (both targeted by DDdCas9VP192), and their downstream targets NKX2.2 and SOX9. Scale bars represent 200 μm.
(E) qRT-PCR analysis of cells treated as in (D) at day 3 of differentiation. Data represent mean ± SEM, n = 3 independently treated samples.
(F) Schematic representation of hPSC differentiation toward pancreatic progenitors using two inducible systems at different time points: TMP-inducible DDdCas9VP192 activating PDX1 and NKX6.1 endogenous expression (days 3 to 9) and DOX-inducible TetON-MAFA-ires-GFP overexpression system (days 7 to 9).
(G) qRT-PCR analysis of experiment depicted in (F). *PDX1* and *NKX6.1* expression levels are shown at days 7 and 9 in −/+ TMP-treated samples. *MAFA* and its downstream target *GCK* expression levels are shown at days 7 and 9 in −/+ DOX-treated samples. Data represent mean ± SEM, n = 3 independently treated samples.
(H) Immunocytochemistry for NKX6.1 and MAFA of hESC treated as depicted in (F). Scale bars represent 200 μm.

College of Medicine) for advice on Golden Gate cloning. This study was supported by the Tekes Large Strategic Research Opening 3i Regeneration (project number 40395/13), the Academy of Finland, the Sigrid Juselius Foundation, the Novo Nordisk Foundation, and the Instrumentarium Science Foundation. D.B. and J.W. are supported by the Doctoral Program in Biomedicine, University of Helsinki.

Received: November 20, 2014
Revised: August 1, 2015
Accepted: August 3, 2015
Published: September 8, 2015

REFERENCES

Arda, H.E., Benitez, C.M., and Kim, S.K. (2013). Gene regulatory networks governing pancreas development. Dev. Cell *25*, 5–13.

Baron, U., Gossen, M., and Bujard, H. (1997). Tetracycline-controlled transcription in eukaryotes: novel transactivators with graded transactivation potential. Nucleic Acids Res. *25*, 2723–2729.

Bikard, D., Jiang, W., Samai, P., Hochschild, A., Zhang, F., and Marraffini, L.A. (2013). Programmable repression and activation of bacterial gene expression using an engineered CRISPR-Cas system. Nucleic Acids Res. *41*, 7429–7437.

Chakraborty, S., Ji, H., Kabadi, A.M., Gersbach, C.A., Christoforou, N., and Leong, K.W. (2014). A CRISPR/Cas9-based system for reprogramming cell lineage specification. Stem Cell Reports *3*, 940–947.

Chavez, A., Scheiman, J., Vora, S., Pruitt, B.W., Tuttle, M., P R Iyer, E., Lin, S., Kiani, S., Guzman, C.D., Wiegand, D.J., et al. (2015). Highly efficient Cas9-mediated transcriptional programming. Nat. Methods *12*, 326–328.

Cheng, A.W., Wang, H., Yang, H., Shi, L., Katz, Y., Theunissen, T.W., Rangarajan, S., Shivalila, C.S., Dadon, D.B., and Jaenisch, R. (2013). Multiplexed activation of endogenous genes by CRISPR-on, an RNA-guided transcriptional activator system. Cell Res. *23*, 1163–1171.

Cong, L., Ran, F.A., Cox, D., Lin, S., Barretto, R., Habib, N., Hsu, P.D., Wu, X., Jiang, W., Marraffini, L.A., and Zhang, F. (2013). Multiplex genome engineering using CRISPR/Cas systems. Science *339*, 819–823.

Davis, K.M., Pattanayak, V., Thompson, D.B., Zuris, J.A., and Liu, D.R. (2015). Small molecule-triggered Cas9 protein with improved genome-editing specificity. Nat. Chem. Biol. *11*, 316–318.

Esvelt, K.M., Mali, P., Braff, J.L., Moosburner, M., Yaung, S.J., and Church, G.M. (2013). Orthogonal Cas9 proteins for RNA-guided gene regulation and editing. Nat. Methods *10*, 1116–1121.

Gao, X., Tsang, J.C.H., Gaba, F., Wu, D., Lu, L., and Liu, P. (2014). Comparison of TALE designer transcription factors and the CRISPR/dCas9 in regulation of gene expression by targeting enhancers. Nucleic Acids Res. *42*, e155.

Gilbert, L.A., Larson, M.H., Morsut, L., Liu, Z., Brar, G.A., Torres, S.E., Stern-Ginossar, N., Brandman, O., Whitehead, E.H., Doudna, J.A., et al. (2013). CRISPR-mediated modular RNA-guided regulation of transcription in eukaryotes. Cell *154*, 442–451.

Gilbert, L.A., Horlbeck, M.A., Adamson, B., Villalta, J.E., Chen, Y., Whitehead, E.H., Guimaraes, C., Panning, B., Ploegh, H.L., Bassik, M.C., et al. (2014). Genome-Scale CRISPR-Mediated Control of Gene Repression and Activation. Cell *159*, 647–661.

Hilton, I.B., D'Ippolito, A.M., Vockley, C.M., Thakore, P.I., Crawford, G.E., Reddy, T.E., and Gersbach, C.A. (2015). Epigenome editing by a CRISPR-Cas9-based acetyltransferase activates genes from promoters and enhancers. Nat. Biotechnol. *33*, 510–517.

Hu, J., Lei, Y., Wong, W.-K., Liu, S., Lee, K.-C., He, X., You, W., Zhou, R., Guo, J.-T., Chen, X., et al. (2014). Direct activation of human and mouse Oct4 genes using engineered TALE and Cas9 transcription factors. Nucleic Acids Res. *42*, 4375–4390.

Iwamoto, M., Björklund, T., Lundberg, C., Kirik, D., and Wandless, T.J. (2010). A general chemical method to regulate protein stability in the mammalian central nervous system. Chem. Biol. *17*, 981–988.

Jinek, M., Chylinski, K., Fonfara, I., Hauer, M., Doudna, J.A., and Charpentier, E. (2012). A programmable dual-RNA-guided DNA endonuclease in adaptive bacterial immunity. Science *337*, 816–821.

Kabadi, A.M., Ousterout, D.G., Hilton, I.B., and Gersbach, C.A. (2014). Multiplex CRISPR/Cas9-based genome engineering from a single lentiviral vector. Nucleic Acids Res. *42*, e147.

Kearns, N.A., Genga, R.M., Enuameh, M.S., Garber, M., Wolfe, S.A., and Maehr, R. (2014). Cas9 effector-mediated regulation of transcription and differentiation in human pluripotent stem cells. Development *141*, 219–223.

Konermann, S., Brigham, M.D., Trevino, A.E., Joung, J., Abudayyeh, O.O., Barcena, C., Hsu, P.D., Habib, N., Gootenberg, J.S., Nishimasu, H., et al. (2015). Genome-scale transcriptional activation by an engineered CRISPR-Cas9 complex. Nature *517*, 583–588.

Maeder, M.L., Linder, S.J., Cascio, V.M., Fu, Y., Ho, Q.H., and Joung, J.K. (2013a). CRISPR RNA-guided activation of endogenous human genes. Nat. Methods *10*, 977–979.

Maeder, M.L., Linder, S.J., Reyon, D., Angstman, J.F., Fu, Y., Sander, J.D., and Joung, J.K. (2013b). Robust, synergistic regulation of human gene expression using TALE activators. Nat. Methods *10*, 243–245.

Mali, P., Esvelt, K.M., and Church, G.M. (2013a). Cas9 as a versatile tool for engineering biology. Nat. Methods *10*, 957–963.

Mali, P., Aach, J., Stranges, P.B., Esvelt, K.M., Moosburner, M., Kosuri, S., Yang, L., and Church, G.M. (2013b). CAS9 transcriptional activators for target specificity screening and paired nickases for cooperative genome engineering. Nat. Biotechnol. *31*, 833–838.

Okita, K., Matsumura, Y., Sato, Y., Okada, A., Morizane, A., Okamoto, S., Hong, H., Nakagawa, M., Tanabe, K., Tezuka, K., et al. (2011). A more efficient method to generate integration-free human iPS cells. Nat. Methods *8*, 409–412.

Perez-Pinera, P., Kocak, D.D., Vockley, C.M., Adler, A.F., Kabadi, A.M., Polstein, L.R., Thakore, P.I., Glass, K.A., Ousterout, D.G., Leong, K.W., et al. (2013). RNA-guided gene activation by CRISPR-Cas9-based transcription factors. Nat. Methods *10*, 973–976.

Qi, L.S., Larson, M.H., Gilbert, L.A., Doudna, J.A., Weissman, J.S., Arkin, A.P., and Lim, W.A. (2013). Repurposing CRISPR as an RNA-guided platform for sequence-specific control of gene expression. Cell *152*, 1173–1183.

Ran, F.A., Cong, L., Yan, W.X., Scott, D.A., Gootenberg, J.S., Kriz, A.J., Zetsche, B., Shalem, O., Wu, X., Makarova, K.S., et al. (2015). In vivo genome editing using Staphylococcus aureus Cas9. Nature *520*, 186–191.

Rezania, A., Bruin, J.E., Arora, P., Rubin, A., Batushansky, I., Asadi, A., O'Dwyer, S., Quiskamp, N., Mojibian, M., Albrecht, T., et al. (2014). Reversal of diabetes with insulin-producing cells derived in vitro from human pluripotent stem cells. Nat. Biotechnol. *32*, 1121–1133.

Sakuma, T., Nishikawa, A., Kume, S., Chayama, K., and Yamamoto, T. (2014). Multiplex genome engineering in human cells using all-in-one CRISPR/Cas9 vector system. Sci. Rep. *4*, 5400.

Shalem, O., Sanjana, N.E., Hartenian, E., Shi, X., Scott, D.A., Mikkelsen, T.S., Heckl, D., Ebert, B.L., Root, D.E., Doench, J.G., and Zhang, F. (2014). Genome-scale CRISPR-Cas9 knockout screening in human cells. Science *343*, 84–87.

Tanenbaum, M.E.E., Gilbert, L.A.A., Qi, L.S.S., Weissman, J.S.S., and Vale, R.D.D. (2014). A protein-tagging system for signal amplification in gene expression and fluorescence imaging. Cell *159*, 635–646.

Vuoristo, S., Toivonen, S., Weltner, J., Mikkola, M., Ustinov, J., Trokovic, R., Palgi, J., Lund, R., Tuuri, T., and Otonkoski, T. (2013). A novel feeder-free culture system for human pluripotent stem cell culture and induced pluripotent stem cell derivation. PLoS ONE *8*, e76205.

Wang, H., Brun, T., Kataoka, K., Sharma, A.J., and Wollheim, C.B. (2007). MAFA controls genes implicated in insulin biosynthesis and secretion. Diabetologia *50*, 348–358.

Wang, T., Wei, J.J., Sabatini, D.M., and Lander, E.S. (2014). Genetic screens in human cells using the CRISPR-Cas9 system. Science *343*, 80–84.

Yu, J., Hu, K., Smuga-Otto, K., Tian, S., Stewart, R., Slukvin, I.I., and Thomson, J.A. (2009). Human induced pluripotent stem cells free of vector and transgene sequences. Science *324*, 797–801.

Zetsche, B., Volz, S.E., and Zhang, F. (2015). A split-Cas9 architecture for inducible genome editing and transcription modulation. Nat. Biotechnol. *33*, 139–142.

Stem Cell Reports, Volume *5*

Supplemental Information

Conditionally Stabilized dCas9 Activator for Controlling Gene Expression in Human Cell Reprogramming and Differentiation

Diego Balboa, Jere Weltner, Solja Eurola, Ras Trokovic, Kirmo Wartiovaara, and Timo Otonkoski

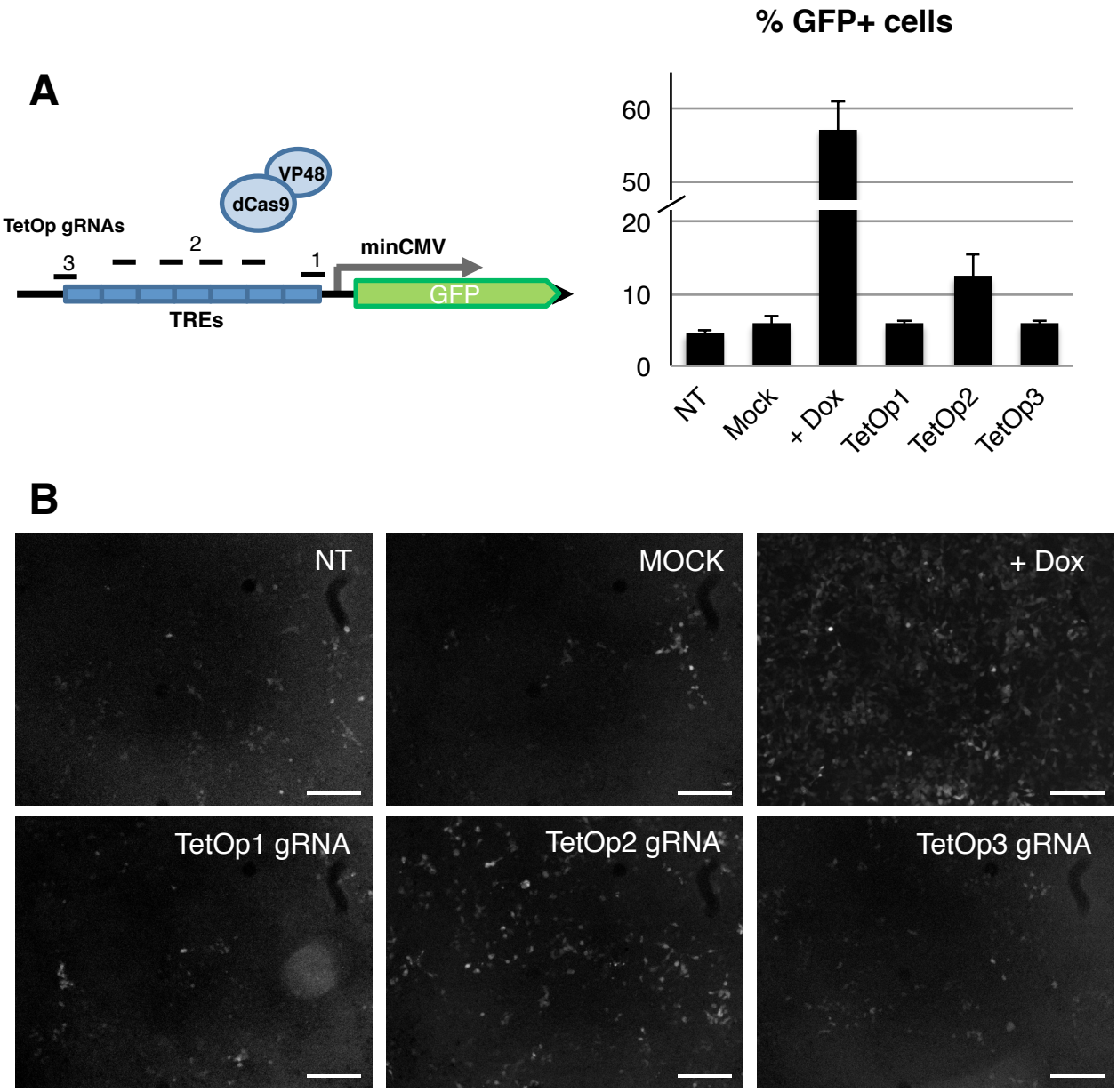

Figure S1. Validation of dCas9VP48 activator. Related to Figure 1.

(A) dCas9VP48 construct was transfected together with gRNAs targeting the tetracycline response element (TRE) repeats in the Tet-ON promoter. Number of GFP+ HEK293 cells was analyzed by flow cytometry. Data represent mean ± SEM, n = 3 independent transfections. Addition of doxycycline (+Dox) to activate rtTA-mediated GFP-expression was used as a positive control and non-transfected (NT) and dCas9VP48-only transfected (Mock) were used as negative controls.
(B) Representative fluorescence microscopy fields of GFP+ cells in the different conditions. Scale bars 200 μm.

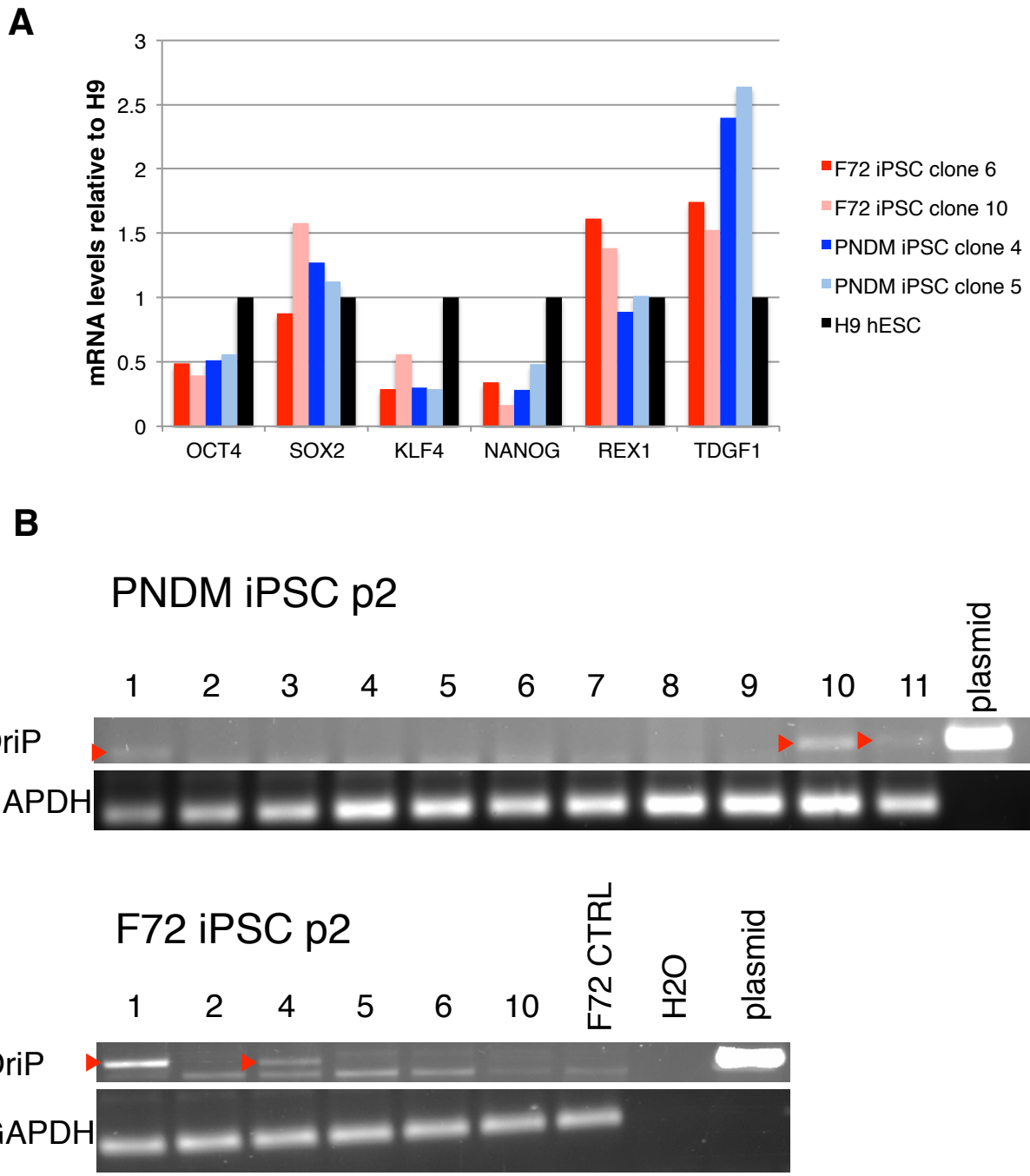

Figure S2. Characterization of dCasVP192 OCT4 reprogrammed iPSC. Related to Figure 2.

(A) qRT-PCR characterization of reprogrammed iPSC clones. mRNA levels of pluripotency markers relative to H9.
(B) Episome detection PCR of DNA preparations from dCasVP192 OCT4 reprogrammed iPSC. Red arrows indicate persistent or integrated plasmids in assayed clones.

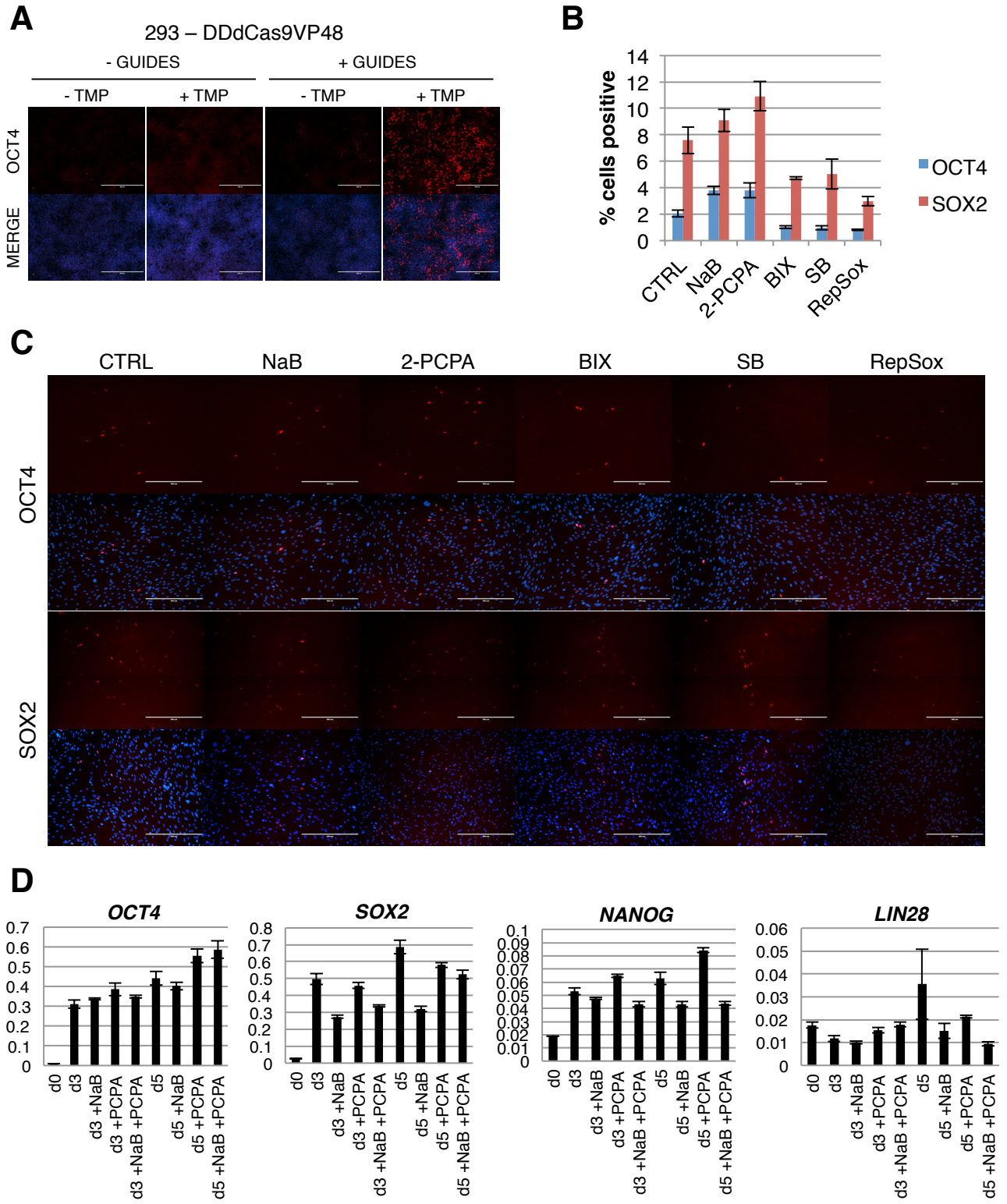

Figure S3. Effect of small molecular compounds on human fibroblast gene activation. Related to Figure 3.

(A) TMP dependent *OCT4* activation in HEK293 cells expressing DDdCas9VP48 and OCT4 targeting guides. Scale bars = 400 μm in A and C.

(B)(C) Number of OCT4 and SOX2 positive cells counted per visual field and representative immunocytochemical stainings of F72 fibroblasts expressing DDdCas9VP192 and *OCT4*, *SOX2*, *NANOG* and *LIN28A* targeting guides and treated with TMP and inhibitors. NaB = sodium butyrate, 2-PCPA = *trans*-2-Phenylcyclopropylamine (Tranylcypromine), BIX = BIX01294, SB = SB431542.

(D) Activation of *OCT4, SOX2 NANOG* and *LIN28A* by qPCR in the presence of 250 μM NaB and 4 μM PCPA after 3 and 5 days of 1 μM TMP treatment in F72 expressing DDdCas9VP192 and OCT4, SOX2, NANOG and LIN28A targeting guides. Data represented as mean ±SEM, n=3.

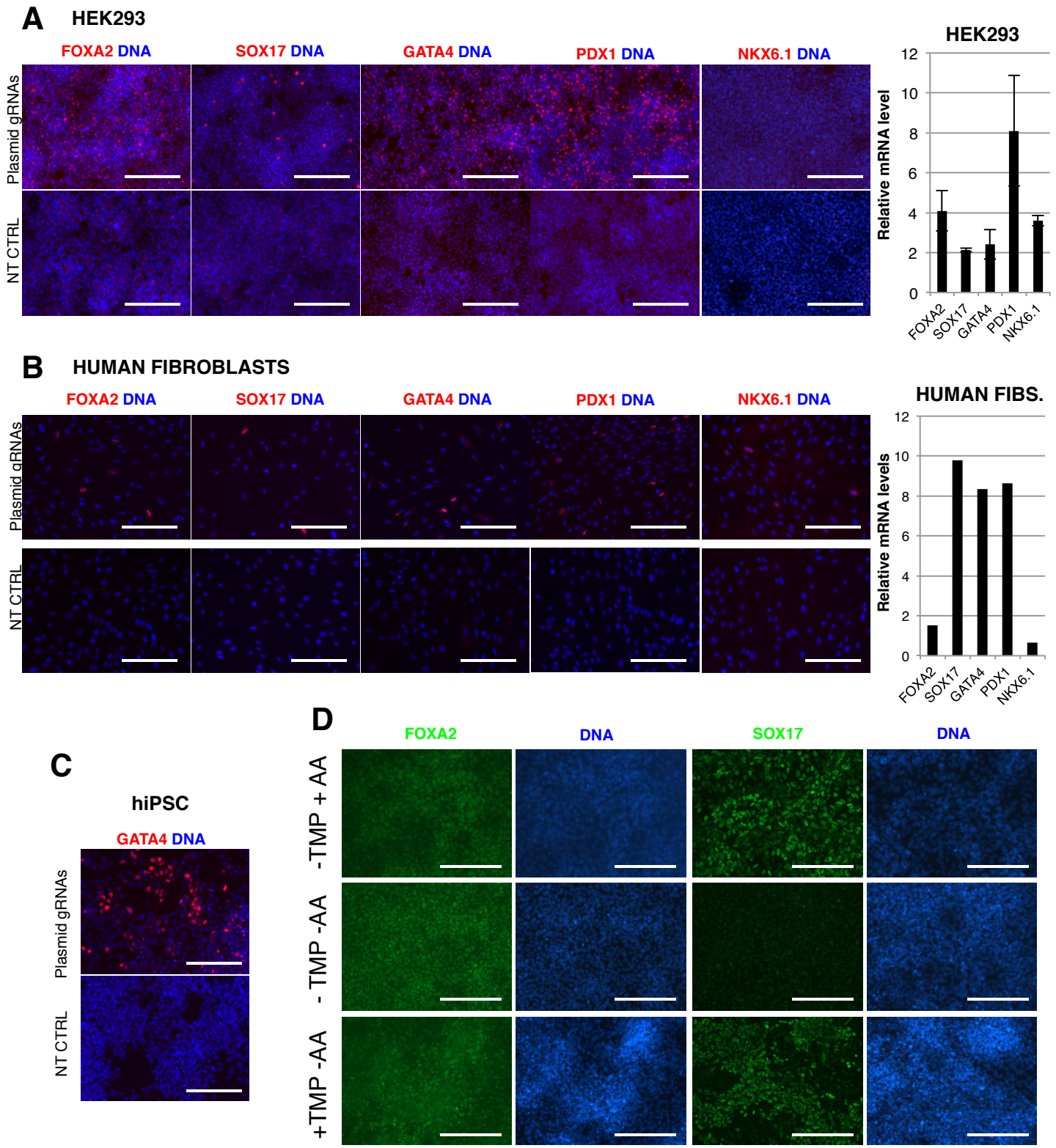

Figure S4. Activation of endodermal lineage specific transcription factors by dCas9VP192 mediated transcriptional activation. Related to Figure 4.

(A)(B) Immunocytochemical detection and qPCR analyses of indicated targeted gene products in HEK293 and F72 human foreskin fibroblasts. Analysis was performed 72 h after delivery of gRNA-concatenated plasmids and dCas9VP192. mRNA levels relative to non-treated cells, represented as mean ± SD, n=2 for HEK293 and n=1 for F72. Scale bars = 200 μm for all panels.
(E) Immunocytochemical detection of GATA4 in hiPSC transfected with dCas9VP192 and gRNAS.
(D) Immunocytochemical detection of FOXA2 and SOX17 in hESC expressing DDdCas9VP192 and gRNAs for FOXA2, SOX17, PDX1 and NKX6.1 differentiated to definitive endoderm at day 3.

Supplemental Experimental Procedures

Plasmid construction

Catalytically inactive dCas9 was cloned by introducing H840A mutation by PCR into pX334-U6-DR-BB-DR-Cbh-NLS-hSpCas9n(D10A)-NLS-H1-shorttracr-PGK-puro (pX334) (Addgene plasmid: 42333) (Cong et al., 2013). The dCas9 construct was cloned into pX335-U6-Chimeric_BB-CBh-hSpCas9n(D10A) (Addgene plasmid: 42335) along with PKG Puro from pX334 to create pX335-U6-Chimeric_BB-CBh-dCas9-PGK-Puro. VP16 transactivation domain repeats were cloned from rtTA by PCR and fused C-terminally to dCas9 in pX335-U6-Chimeric_BB-CBh-dCas9-PGK-Puro to create dCas9 transactivator constructs. T2A-GFP was fused C-terminally to dCas9VP192 and cloned into CAG-IRES-Puro backbone to create CAG-dCas9VP192-GFP-Puro construct. For episomal replicating plasmids dCas9VP192-GFP fragment was cloned from CAG-dCas9VP192-GFP-Puro into pCXLE backbone (pCXLE-hSK; Addgene plasmid: 27078; Okita et al., 2011) with EcoRI. pCXLE-dCas9VP192-GFP-shp53 was cloned by inserting dCas9VP192-GFP into backbone from pCXLE-hOCT3/4-shp53-F (Addgene plasmid: 27077). pCXLE-hOCT4 was cloned form pCXLE-hOCT3/4-shp53 by removing the p53 shRNA sequence between BamHI sites. PiggyBac constructs encoding the dCas9VP192-GFP-IRES-Neo were cloned by inserting the CAG dCas9 activator between PiggyBac recombination sites in pPB-R1R2-NeoPheS (Yusa et al., Nature, 2011). Destabilized dCas9 activator was generated by PCR cloning the DHFR(DD) from pBMN DHFR(DD)-YFP (Addgene plasmid: 29352) and inserting it N-terminally in fusion with the dCas9 in the PB-CAG-dCas9VP192-GFP-IRES-Neo. MAFA overexpression construct was generated by PCR cloning the human MAFA cDNA into PB-tight-ires-EmGFP backbone.

Guide RNA production

Guide RNA transcriptional units (gRNA-PCR) were prepared by PCR amplification with Phusion polymerase (ThermoFisher), using as template U6 promoter and terminator PCR products amplified from pX335 together with a guide RNA sequence-containing oligo to bridge the gap. PCR reaction contained 50 pmol forward (Fw) and reverse (Rev) primers, 2 pmol guide oligo, 5 ng U6 promoter and 5 ng terminator PCR products in a total reaction volume of 100μl. PCR reaction program was 98C/10sec, 56C/30sec, 72C/12sec for 35 cycles. Amplified gRNA-PCRs were purified and confirmed by sequencing. When needed, alternative Fw and Rev primers were used to incorporate suitable restriction sites for gRNA-PCR concatenation.

gRNA-PCR units were concatenated using Golden Gate assembly (Cermak et al., 2011) . Destination vector GGdest-ready was generated by PCR-cloning Esp3I destination cassette from pCAG-T7-TALEN(Sangamo)-Destination (Addgene plasmid: 37184; (Hermann et al., 2014) into pGEM-4Z (Promega). Assembly reactions contained 150 ng of GGdest-ready vector, 50 ng of each gRNA-PCR product (five in total), 1 uL Esp3I (Thermo Fisher, ER0451), 2 uL T4 DNA ligase (Thermo Fisher, EL0011), 2 uL T4 ligase buffer and 2 uL DTT (10mM, Promega, V3151) in a final volume of 20 uL. Thermal cycle consisted of 50 cycles of restriction/ligation (2 min at 37°C, 5 min at 16°C) followed by enzyme inactivation step (20 min at 80ºC). Ten microliters of the reaction were transformed into DH5alpha chemical competent bacteria and plated on LB agar containing ampicillin with IPTG/X-Gal for blue/white recombinant screening. Correct concatenation of the gRNA-PCR products was confirmed by sequencing.

gRNAs concatenated into the GGdest-ready were further cloned into either EBNA or PiggyBac backbones for the different experiments.

Cell transfection

HEK293 cells were seeded on tissue culture treated 24 well plates one day prior to transfection (10^5 cells/well). hESC and hiPSC cells were split to Matrigel-coated 24-well plates 48 hours before transfection. Cells were transfected using FuGENE HD transfection reagent (Promega) in fibroblast culture medium or E8 stem cell media with 500 ng of dCas9 transactivator encoding plasmid and 100 to 200 ng of gRNA-PCR or 500 ng gRNA-PCR. Cells were cultured for 72 hours post-transfection, after which samples were collected for FACS analysis, qRT-PCR or immunocytochemical staining.

Cell electroporation

Human skin fibroblasts were electroporated using Neon Transfection system (Life Technologies) according to manufacturer's instructions. Briefly, 1 million cells were electroporated in 100 μl tips with 1650 V, 10 ms and 3x pulse settings. Amounts of DNA used were: 6 μg of total plasmid consisting of 3 μg of guide template EBNA plasmids and 3 μg of pCXLE-dCas9VP192-GFP-shp53 per electroporation. For OCT4 replacement experiments 2μg of pCXLE-dCas9VP192-GFP-shp53, 2μg of OCT4 gRNA plasmid, 1μg of pCXLE-hSK and 1μg of pCXLE-hUL were used. For transgenic OCT4 control OCT4 gRNA plasmid was replaced with pCXLE-hOCT3/4-shp53 (2μg) and dCas9VP192 plasmid was replaced with pCXLE-GFP (2μg). For selected inducible cell lines fibroblasts were electroporated with 1μg of PB-transposase, 2μg of PB-CAG-DDdCas9VP192-GFP-IRES-Neo, 1.5μ of PB-OCT4-SOX2-guides-PGK-Puro and 1.5μg of PB-NANOG-LIN28A-guides-

PGK-Puro plasmids. After electroporation cells were plated in fibroblast medium on gelatin-coated tissue culture plates and selected with G418 (Roche) and puromycin (Life Technologies).

For the generation of the hESC line used in the differentiation experiments, 2 million H9 (WiCell) cells were electroporated with 2 μg of PB-CAG-DDdCas9VP192-GFP-IRES-Neo, 1 μg PB-FOXA2-SOX17-guides-PGK-Puro, 1 μg PB-PDX1-NKX6.1-guides-PGK-Puro and 1μg of PB-transposase using Neon Transfection system (1100 V, 20 ms, 2x pulses). Cells were plated onto a Matrigel coated plate with E8 medium containing 5 uM ROCK inhibitor (Y-27632 2HCl, Selleckchem). 72 h after electroporation and recovery cells were selected with G418 and puromycin.

hESC differentiation to endoderm and pancreatic lineage

hESC expansion and plating, and media used for differentiation to definitive endoderm was performed as described in Rezania et al., 2014. Briefly, confluent plates of H9 hESC cells were washed twice with PBS and incubated for 72 h in the following endoderm differentiation media: d0: MCDB131 (Life Technologies) + 2mM Glutmax (Life Technologies) + 1.5 g/L NaHCO3 (Sigma) + 0.5% BSA fV (Sigma) + 10mM final Glucose (Sigma) + 100 ng/ml Activin A (Dr Marko Hyvonen, Department of Biochemistry, University of Cambridge) + 3 μM CHIR; d1: Identical to d0 but only 0.3 μM CHIR; d2: Identical to d0 but no CHIR. After definitive endoderm stage, cells were differentiated to pancreatic progenitors as described in Rezania et al., 2014 .

Immunocytochemistry

Cells were fixed with 4% paraformaldehyde (PFA), permeabilized using 0.2% Triton-x100 and blocked using Ultra V Block (Thermo Fisher). Primary antibodies were diluted in PBS

containing 0.1% Tween-20 and incubated overnight in +6°C. Secondary antibody incubations were done in room temperature for half an hour. After antibody incubations, cell nuclei were stained with 4',6-diamidino-2-phenylindole (DAPI) or Hoechst and cells were imaged under fluorescent microscope (EVOS, Life Technologies). Primary antibodies used were: OCT4 (1:500, C30A3, Cell Signaling; 1:100, MA1-104, Thermo; 1:500, SC-8628, Santa Cruz), SOX2 (1:500, D6D9, Cell Signaling), LIN28A (1:500, D84C11, Cell Signaling; 1:100, MA1-016, Thermo), NANOG (1:500, D73G4, Cell Signaling; 1:100, MA1-017, Thermo), E-cadherin (1:500, 610181, BD Bioscience), KLF4 (1:250, HPA002926, Sigma-Aldrich), FOXA2 (1:500, SC-9187, Santa Cruz), PDX1 (1:200, AF2419, R&D Systems), NKX6.1 (1:200, F55A10, Developmental Studies Hybridoma Bank), SOX17 (1:500, AF1924, R&D Systems), GATA4 (1:500, SC-1237, Santa Cruz) and MAFA (1:500, AB26405, Abcam). Secondary antibodies used were AlexaFluor 488/594: donkey anti-goat (1:500, A11055 and A11058; Invitrogen), donkey anti-mouse (1:500, A21202 and A21203; Invitrogen) and donkey anti-rabbit (1:500, A21206 and A21207; Invitrogen). For estimation of activation efficiency from immunostainings cells were manually counted from four random fields per sample.

Flow cytometry

For GFP+ flow cytometry, cells were dissociated using incubation with TrypLE Select (Life Technologies 12563029) for 5 min at 37ºC, counted and resuspended in FACS-buffer (5% FBS in PBS). Samples were run with FACSCalibur (BD Biosciences) and analyzed with CellQuest-Pro software (BD Biosciences). Non-treated cells were used as control for gating.

Quantitative RT-PCR (qRT-PCR) analysis

Gene expression was assessed using SYBR-Green based qRT-PCR, performed as previously described elsewhere (Toivonen et al., 2013). Relative expression was analysed using ΔΔCt method, with cyclophilin G (*PPIG*) as endogenous control and an exogenous positive control used as calibrator. Expression levels are relative to non-treated cells or to hESC as indicated in the figure legends.

Primers for qRT-PCR

Gene	Reference	Forward	Reverse	Product size (bp)
CYCLOG	NM_004792	TCTTGTCAATGGCCAACAGAG	GCCCATCTAAATGAGGAGTTG	84
OCT4	NM_002701	TTGGGCTCGAGAAGGATGTG	TCCTCTCGTTGTGCATAGTCG	91
SOX2	NM_003106	GCCCTGCAGTACAACTCCAT	TGCCCTGCTGCGAGTAGGA	85
NANOG	NM_024865.2	CTCAGCCTCCAGCAGATGC	TAGATTTCATTCTCTGGTTCTGG	94
LIN28	NM_024674	AGGAGACAGGTGCTACAACTG	TCTTGGGCTGGGGTGGCAG	74
KLF4	NM_004235.4	CCGCTCCATTACCAAG	CACGATCGTCTTCCCCTCTT	80
CDH1	NM_004360	ATGAGTGTCCCCCGGTATCT	GGTCAGTATCAGCCGCTTTC	91
FOXA2	NM_021784	AAGACCTACAGGCGCAGCT	CATCTTGTTGGGGCTCTGC	93
SOX17	NM_022454	CCGAGTTGAGCAAGATGCTG	TGCATGTGCTGCACGCGCA	103
GATA4	NM_002052	GAGGAAGGAGCCAGCCTAGCAG	CGGGTCCCCCACTCGTCA	83
PDX1	NM_000209.3	AAGTCTACCAAAGCTCACGCG	CGTAGGCGCCGCCTGC	52
NKX6.1	NM_006168	TATTCGTTGGGGATGACAGAG	TGGCCATCTCGGCAGCGTG	91
NKX2.2	NM_002509	GAACCCCTTCTACGACAGCA	ACCGTGCAGGGAGTACTGAA	82
SOX9	NM_000346	ATCAAGACGGAGCAGCTGAG	GGCTGTAGTGTGGGAGGTTG	100
MAFA	NM_201589	GCCAGGTGGAGCAGCTGAA	CTTCTCGTATTTCTCCTTGTAC	77
GCK	NM_000162	CCGCCAAGAAGGAGAAGGTA	CTTCTGCATCCGTCTCATCA	89

Primers for gRNA amplification and concatenation

U6 promoter fragment PCR	
5pTailedU6promFw	GTAAAACGACGGCCAGTGAGGGCCTATTTCCCATGATTC
U6promRv	GGTGTTTCGTCCTTTCCAC
Terminator fragment PCR	
TermRv80bp	AAAAAAAGCACCGACTCGGTGCCACTTTTTCAAGTTGATAACGGACTAGCCTTATTTTAACTTGCTATTTCTAGCTCTAAAAC
3pTailedTerm80bpRv	AGGAAACAGCTATGACCATGAAAAAAAGCACCGACTCGGTGCCAC
Term80 Fw	GTTTTAGAGCTAGAAATAGCAAG
Golden Gate concatenation	
1_aggc_Fw	ACTGAATTCGGATCCTCGAGCGTCTCACCCTGTAAAACGACGGCCAGT
1_aggc_Rv	CATGCGGCCGCGTCGACAGATCTCGTCTCACATGAGGAAACAGCTATGACCATG
2_aggc_Fw	ACTGAATTCGGATCCTCGAGCGTCTCACATGGTAAAACGACGGCCAGT
3_aggc_Fw	ACTGAATTCGGATCCTCGAGCGTCTCAGGACGTAAAACGACGGCCAGT
4_aggc_Fw	ACTGAATTCGGATCCTCGAGCGTCTCACCAGGTAAAACGACGGCCAGT
5_aggc_Fw	ACTGAATTCGGATCCTCGAGCGTCTCATGTTGTAAAACGACGGCCAGT
2_aggc_Rv	CATGCGGCCGCGTCGACAGATCTCGTCTCAGTCCAGGAAACAGCTATGACCATG
3_aggc_Rv	CATGCGGCCGCGTCGACAGATCTCGTCTCACTGGAGGAAACAGCTATGACCATG
4_aggc_Rv	CATGCGGCCGCGTCGACAGATCTCGTCTCAAACAAGGAAACAGCTATGACCATG
5_aggc_Rv	CATGCGGCCGCGTCGACAGATCTCGTCTCACGTTAGGAAACAGCTATGACCATG
gRNA oligos	
pOct_1	GTGGAAAGGACGAAACACCGGGGGGAGAAACTGAGGCGAGTTTTAGAGCTAGAAATAG
pOct_2	GTGGAAAGGACGAAACACCGGGTGGTGGCAATGGTGTCTGGTTTTAGAGCTAGAAATAG
pOct_3	GTGGAAAGGACGAAACACCGGACACAACTGGCGCCCCTCCGTTTTAGAGCTAGAAATAG

pOct_4	GTGGAAAGGACGAAACACCGGGCACAGTGCCAGAGGTCTGGTTTTAGAGCTAGAAATAG
pOct_5	GTGGAAAGGACGAAACACCGTCTGTGGGGGACCTGCACTGGTTTTAGAGCTAGAAATAG
pNanog1	GTGGAAAGGACGAAACACCGTCCCAATTTACTGGGATTACGTTTTAGAGCTAGAAATAG
pNanog2	GTGGAAAGGACGAAACACCGTGATTTAAAAGTTGGAAACGGTTTTAGAGCTAGAAATAG
pNanog3	GTGGAAAGGACGAAACACCGTCTAGTTCCCCACCTAGTCTGTTTTAGAGCTAGAAATAG
pNanog4	GTGGAAAGGACGAAACACCGGATTAACTGAGAATTCACAAGTTTTAGAGCTAGAAATAG
pNanog5	GTGGAAAGGACGAAACACCGCGCCAGGAGGGGTGGGTCTAGTTTTAGAGCTAGAAATAG
pCDH1_5	GTGGAAAGGACGAAACACCGGAGACAAGTCGGGGCGGACAGTTTTAGAGCTAGAAATAG
pCDH1_4	GTGGAAAGGACGAAACACCGTCAGAAAGGGCTTTTACACTGTTTTAGAGCTAGAAATAG
pCDH1_3	GTGGAAAGGACGAAACACCGGTCTTAGTGAGCCACCGGCGGTTTTAGAGCTAGAAATAG
pCDH1_2	GTGGAAAGGACGAAACACCGCAGTGGAATCAGAACCGTGCGTTTTAGAGCTAGAAATAG
pCDH1_1	GTGGAAAGGACGAAACACCGAGGGTCACCGCGTCTATGCGGTTTTAGAGCTAGAAATAG
pKLF4_5	GTGGAAAGGACGAAACACCGTCTTCGCGGGCTTCGAACCCGTTTTAGAGCTAGAAATAG
pKLF4_4	GTGGAAAGGACGAAACACCGGTTCGGTCGCTGCGCGACCAGTTTTAGAGCTAGAAATAG
pKLF4_3	GTGGAAAGGACGAAACACCGGCTGCCATAGCAACGATGGAGTTTTAGAGCTAGAAATAG
pKLF4_2	GTGGAAAGGACGAAACACCGTATAAGTAAGGAACGCGCGCGTTTTAGAGCTAGAAATAG
pKLF4_1	GTGGAAAGGACGAAACACCGCGAACGTGTCTGCGGGCGCGGTTTTAGAGCTAGAAATAG
pLIN28_5	GTGGAAAGGACGAAACACCGTCTGATTGGCCAGCGCCGCCGTTTTAGAGCTAGAAATAG
pLIN28_4	GTGGAAAGGACGAAACACCGTAATTATCTGCCCGGGGGGTGTTTTAGAGCTAGAAATAG
pLIN28_3	GTGGAAAGGACGAAACACCGCGGGGTACTCAAGTCTTCTAGTTTTAGAGCTAGAAATAG
pLIN28_2	GTGGAAAGGACGAAACACCGCCCATCTCCAGTTGTGCGTGGTTTTAGAGCTAGAAATAG
pLIN28_1	GTGGAAAGGACGAAACACCGGTGTCAGAGACCGGAGTTGTGTTTTAGAGCTAGAAATAG
pSox2_1	GTGGAAAGGACGAAACACCGTGTAAGGTAAGAGAGGAGAGGTTTTAGAGCTAGAAATAG
pSox2_2	GTGGAAAGGACGAAACACCGTTTACCCACTTCCTTCGAAAGTTTTAGAGCTAGAAATAG
pSox2_3	GTGGAAAGGACGAAACACCGGTGGCTGGCAGGCTGGCTCTGTTTTAGAGCTAGAAATAG
pSox2_4	GTGGAAAGGACGAAACACCGCAAAACCCGGCAGCGAGGCTGTTTTAGAGCTAGAAATAG
pSox2_5	GTGGAAAGGACGAAACACCGAGGAGCCGCCGCGCGCTGATGTTTTAGAGCTAGAAATAG
pFoxA2_1	GTGGAAAGGACGAAACACCGAGTGCCGAGCTGCCCCGAGGGTTTTAGAGCTAGAAATAG
pFoxA2_2	GTGGAAAGGACGAAACACCGCGCGCGGCGCGGGGGCTAGTGTTTTAGAGCTAGAAATAG

pFoxA2_3	GTGGAAAGGACGAAACACCGTGCGGCACTTGTCCGCTCCGGTTTTAGAGCTAGAAATAG
pFoxA2_4	GTGGAAAGGACGAAACACCGTATAGCGCGGCGCGCTGGCGGTTTTAGAGCTAGAAATAG
pFoxA2_5	GTGGAAAGGACGAAACACCGAAATGGGCTGCCCCGGGTCTGTTTTAGAGCTAGAAATAG
pPdx_1	GTGGAAAGGACGAAACACCGGCCCCACGTGGTTCAGCCGGGTTTTAGAGCTAGAAATAG
pPdx_2	GTGGAAAGGACGAAACACCGGCCTGGCTGGCCGCACTAAGGTTTTAGAGCTAGAAATAG
pPdx_3	GTGGAAAGGACGAAACACCGAGCAGGTGCTCGCGGGTACCGTTTTAGAGCTAGAAATAG
pPdx_4	GTGGAAAGGACGAAACACCGGTTTGCTGCACACTCCTGAAGTTTTAGAGCTAGAAATAG
pPdx_5	GTGGAAAGGACGAAACACCGGTTTTCGTGAGCGCCCATTTGTTTTAGAGCTAGAAATAG
pNkx6.1_1	GTGGAAAGGACGAAACACCGGTAGCGCACTTTGAACAGCTGTTTTAGAGCTAGAAATAG
pNkx6.1_2	GTGGAAAGGACGAAACACCGAAACTCTCCGGAGCCAGCCTGTTTTAGAGCTAGAAATAG
pNkx6.1_3	GTGGAAAGGACGAAACACCGAGGACGCCTTGTGCAGCCCGGTTTTAGAGCTAGAAATAG
pNkx6.1_4	GTGGAAAGGACGAAACACCGCCGAATCTCCACTTTGAAGTGTTTTAGAGCTAGAAATAG
pNkx6.1_5	GTGGAAAGGACGAAACACCGGCTCTGCTCTTTCGGTCGCGGTTTTAGAGCTAGAAATAG
gSox17_1	GTGGAAAGGACGAAACACCGGGGCGTGGGCCTAACGACGCGTTTAAGAGCTATGCTGGA
gSox17_2	GTGGAAAGGACGAAACACCGGTGGGGTTGGACTGGGACGTGTTTAAGAGCTATGCTGGA
gSox17_3	GTGGAAAGGACGAAACACCGGCTCCGGCTAGTTTTCCCGGGTTTAAGAGCTATGCTGGA
gSox17_4	GTGGAAAGGACGAAACACCGTCGAGTCTCCCTAACCCCGGGTTTAAGAGCTATGCTGGA
gSox17_5	GTGGAAAGGACGAAACACCGGGGCAAGTACGTCGATTCCAGTTTAAGAGCTATGCTGGA
gGATA4_1	GTGGAAAGGACGAAACACCGACCTCCAAGGAATCCGGGGCGTTTTAGAGCTAGAAATAG
gGATA4_2	GTGGAAAGGACGAAACACCGCTCAACTCTCGATCTTGTGTGTTTTAGAGCTAGAAATAG
gGATA4_3	GTGGAAAGGACGAAACACCGCAGCGAACCCAATCGACCTCGTTTTAGAGCTAGAAATAG
gGATA4_4	GTGGAAAGGACGAAACACCGAATGCCCAAGTGCTACCGCCGTTTTAGAGCTAGAAATAG
gGATA4_5	GTGGAAAGGACGAAACACCGCCTGTGGGAGTCACGTGCAAGTTTTAGAGCTAGAAATAG
tetOp1	GTGGAAAGGACGAAACACCGGTACCTTCTCTATCACTGATGTTTTAGAGCTAGAAATAG
tetOp2	GTGGAAAGGACGAAACACCGGGACTTCTCTATCACTGATAGTTTTAGAGCTAGAAATAG
tetOp3	GTGGAAAGGACGAAACACCGGGGGAGACGTGCGGCCAGCTGTTTTAGAGCTAGAAATAG

Supplemental References

Cermak, T., Doyle, E.L., Christian, M., Wang, L., Zhang, Y., Schmidt, C., Baller, J. a, Somia, N. V, Bogdanove, A.J., and Voytas, D.F. (2011). Efficient design and assembly of custom TALEN and other TAL effector-based constructs for DNA targeting. Nucleic Acids Res. *39*, e82.

Cong, L., Ran, F.A., Cox, D., Lin, S., Barretto, R., Habib, N., Hsu, P.D., Wu, X., Jiang, W., Marraffini, L.A., et al. (2013). Multiplex genome engineering using CRISPR/Cas systems. Science *339*, 819–823.

Hermann, M., Cermak, T., Voytas, D.F., and Pelczar, P. (2014). Mouse genome engineering using designer nucleases. J. Vis. Exp. *86*.

Okita, K., Matsumura, Y., Sato, Y., Okada, A., Morizane, A., Okamoto, S., Hong, H., Nakagawa, M., Tanabe, K., Tezuka, K., et al. (2011). A more efficient method to generate integration-free human iPS cells. Nat. Methods *8*, 409–412.

Rezania, A., Bruin, J.E., Arora, P., Rubin, A., Batushansky, I., Asadi, A., O'Dwyer, S., Quiskamp, N., Mojibian, M., Albrecht, T., et al. (2014). Reversal of diabetes with insulin-producing cells derived in vitro from human pluripotent stem cells. Nat. Biotechnol. *32*, 1121–1133.

Toivonen, S., Lundin, K., Balboa, D., Ustinov, J., Tamminen, K., Palgi, J., Trokovic, R., Tuuri, T., and Otonkoski, T. (2013). Activin A and Wnt-dependent specification of human definitive endoderm cells. Exp. Cell Res. *319*, 2535–2544.